14

Computed Tomography Evaluation in Valvular Heart Disease

Javier Sanz, Leticia Fernández-Friera, and Mario J. García

Introduction

Valvular heart disease (VHD) affects 2.5% of US adults and predominantly involves the left-sided cardiac structures. Regurgitant lesions are more common than stenoses, and mitral regurgitation (MR) is the most prevalent abnormality [1]. Doppler echocardiography is the initial imaging modality of choice, allowing for a complete diagnosis in the majority of patients [2]. In cases of poor acoustic window and/or disparate results regarding disease severity, additional tests may be required. Cardiac catheterization is a time-honored modality, but limited by its invasive nature. Magnetic resonance imaging (MRI) has become an excellent noninvasive alternative for both valvular insufficiency and stenosis [3]. Due to the need for radiation and contrast, computed tomography (CT) has a limited role for the evaluation of VHD as the primary indication. It may occasionally be employed as such when echocardiographic results are inconclusive and the patient is not a good candidate for MRI. However, CT is increasingly used for noninvasive coronary angiography, and useful information on valve anatomy and function can simultaneously be obtained from a coronary examination. Also, in patients with primary valve diseases, ruling out obstructive coronary artery disease is deemed a highly appropriate indication and may allow patients to forgo invasive coronary angiography.

General Considerations

A diagram summarizing the potential applications of CT for the evaluation of patients with VHD is shown in (Figure 14.1). Valvular assessment includes the detection of calcification in noncontrast scans and of other aspects of valvular anatomy and cardiac function using contrast enhancement. Quantification of valve calcification follows the same principles as coronary calcium scoring, and the "Agatston," volumetric and mass scores have been proposed. Electron-beam CT (EBCT) has been traditionally the reference standard for coronary calcium quantification, although multidetector CT (MDCT), particularly using scanners with ≥16 slices, has proven comparable in terms of accuracy and reproducibility. Regarding contrast-enhanced CT, detailed evaluation of valvular function and anatomy is possible for both regurgitant and, particularly, stenotic lesions (planimetry of the valve area). Visualization is usually better with MDCT due to its superior spatial resolution and the ability to image all phases of the cardiac cycle with the use of retrospective electrocardiographic (ECG) gating.

CT allows for accurate quantification of ventricular volumes, ejection fraction, and mass [4], all of which carry important prognostic and therapeutic implications in patients with VHD [2]. In isolated regurgitant lesions, the regurgitant volume (and fraction) can be derived from the

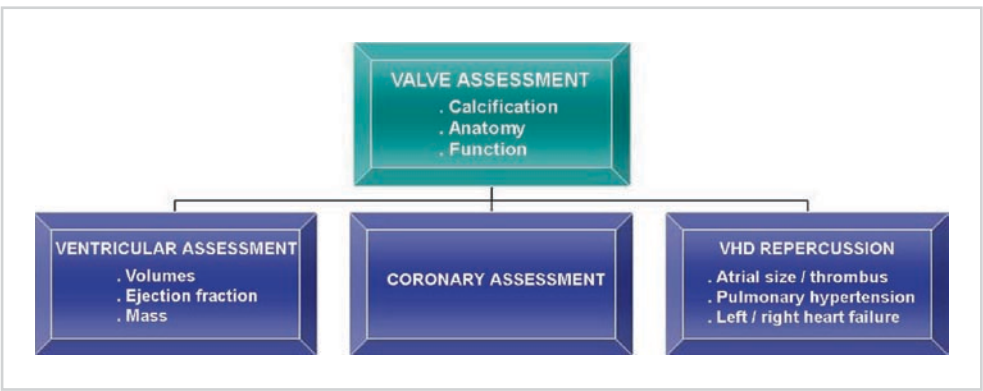

Figure 14.1. Comprehensive evaluation of valvular heart disease (VHD) with CT.

difference between the left and right stroke volumes [5]. Stenosis or regurgitation of the atrioventricular valves usually results in atrial enlargement. Significant regurgitation of any valve eventually causes ipsilateral ventricular dilatation, often accompanied by eccentric hypertrophy. Stenotic lesions of the semilunar (aortic and pulmonary) valves lead to concentric hypertrophy and later may also lead to ventricular dilatation. Poststenotic dilatation of the pulmonary trunk or the ascending aorta may be present as well.

CT can provide important information regarding hemodynamic repercussions of valvular lesions. Enlargement of the right heart chambers can be caused by tricuspid/pulmonary abnormalities or secondary pulmonary hypertension, and typically leads to posterior rotation of the cardiac axis (Figure 14.2). Pulmonary vein dilatation and interstitial and alveolar lung edema are all signs of increased left atrial pressures and left-sided heart failure. Similarly, dilatation of the pulmonary arteries, right heart chambers, superior and inferior vena cava, pleuro-pericardial effusions, and ascitis are suggestive of pulmonary hypertension and/or right ventricular heart failure [6].

CT coronary angiography for preoperative evaluation in VHD is increasingly used, and high accuracy for the detection of significant coronary stenoses has been reported, with slightly lower diagnostic yield in cases of aortic stenosis (AS) due to frequent aortic and coronary calcifications [7–10]. These studies have demonstrated high negative and moderate positive predictive value; thus, patients referred for valvular surgery without significant coronary stenoses by CT may safely avoid the need for invasive angiography [11]. On the other hand, patients with greater than mild degree of luminal stenosis (>50% on CCTA) or extensive calcifications (coronary calcium score >1,000) need to have a confirmatory catheterization. For this reason, it seems prudent to consider CT for this application only in selected patients with low or intermediate pretest probability.

Table 14.1. Imaging protocol

Scanning protocol (for a 256-slice scanner)	
Tube voltage (kV)	100–120
Tube output (mA)	500–800
Detector number	128
Detector collimation (mm)	0.6
ECG gating	Retrospective/prospective
Helical pitch[a]	0.16–0.18
Rotation time (ms)	270–330
Tube current modulation[a]	
(HR ≤ 65)	On
(HR > 65)	Off
Contrast protocol (370 mgI/mL)	
Contrast amount (mL)	80–100
Contrast infusion rate (mL/s)	4–5
Saline amount (mL)	50
Saline infusion rate (mL/s)	4–5
Image reconstruction	
Reconstruction filter	Intermediate
Slice width (mm)	0.6
Increment (mm)	0.3
Matrix	512 × 512
Reconstruction interval[a]	Every 10%
Image analysis: Axial images, MPR, MIP (cine loops and still frames)	

Typical scanning protocol for MDCT coronary angiography employed in our institution (Brilliance *iCT*®, Philips Medical Systems)

ECG electrocardiogram; *HR* heart rate; *MPR* multiplanar reformation; *MIP* maximum intensity projection

[a]If retrospective gating

A typical imaging protocol is summarized in Table 14.1. Contrast infusion is routinely followed by saline, resulting in a more compact bolus and easier evaluation of the right coronary artery; however, it may also impair the visualization of right chambers and valves. This can be overcome by employing a dual- or triple-phase injection protocols [12, 13]. Retrospective ECG gating is advantageous in patients with

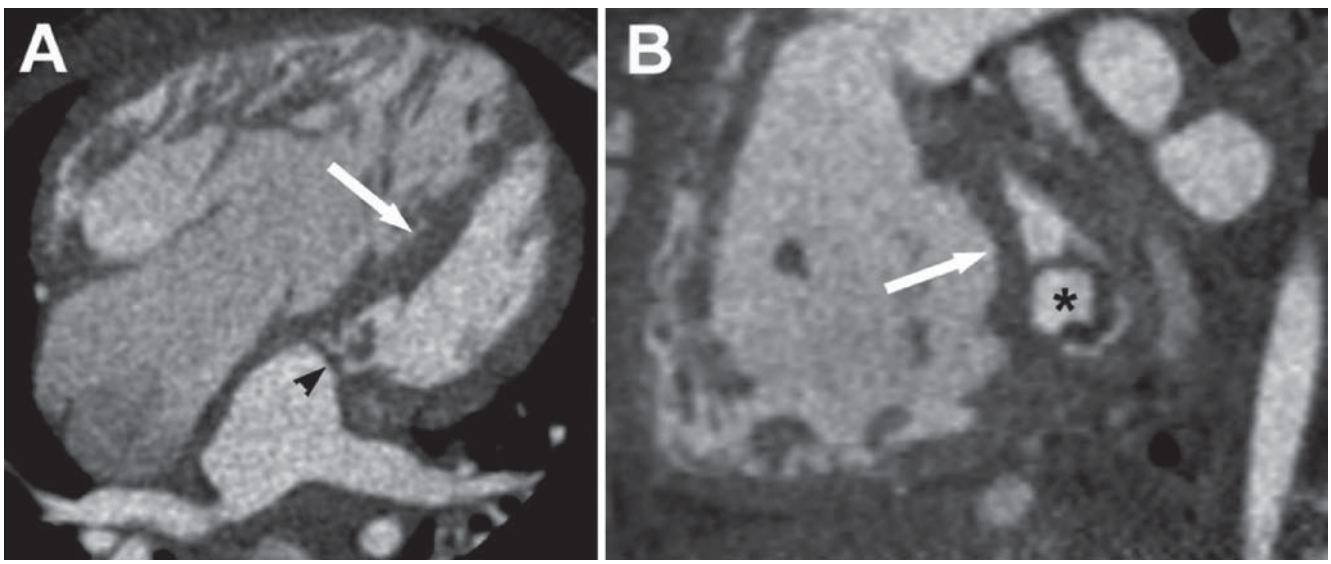

Figure 14.2. Four chamber (**a**) and short-axis (**b**) views of a contrast-enhanced CT scan in a young patient with congenital mitral stenosis ("parachute mitral valve"; *arrowhead* and *asterisk*) and secondary pulmonary hypertension. There is severe right ventricular hypertrophy and enlargement, together with abnormal interventricular septal bowing indicative of right ventricular pressure/volume overload (*arrows*).

VHD at the expense of higher radiation dose. ECG-based tube current modulation can be used, but it may limit the assessment of both ventricles and valves, particularly in obese patients and in the cardiac phases with lower output. If such evaluation is intended, it may be necessary to avoid its use.

Specific Valvular Abnormalities

Aortic Stenosis

Aortic stenosis (AS) is often accompanied by cusp calcification and tends to occur in patients with tri-leaflet valves above 65 years of age or in younger patients with congenital abnormalities (i.e., bicuspid valves). Severe calcification is associated with faster rate of stenosis progression and increased cardiac event rates [14]. Aortic valve calcification can be accurately quantified using CT (Figure 14.3), and interscan reproducibility is >90% [15–17]. The amount of calcification is directly correlated with the severity of AS [17–20], although the relationship is curvilinear (stenosis severity increases more rapidly at lower than higher calcium loads). The incremental value of the information derived from the aortic valve calcium score may be particularly useful in patients with low cardiac output and reduced transvalvular gradients.

Contrast-enhanced CT can precisely evaluate valve morphology, accurately differentiating tri-leaflet from bicuspid valves (Figures 14.4a, b). Planimetric determinations of the aortic valve area (Figure 14.4c) have shown excellent correlation with echocardiographic and invasive measurements [20–27].

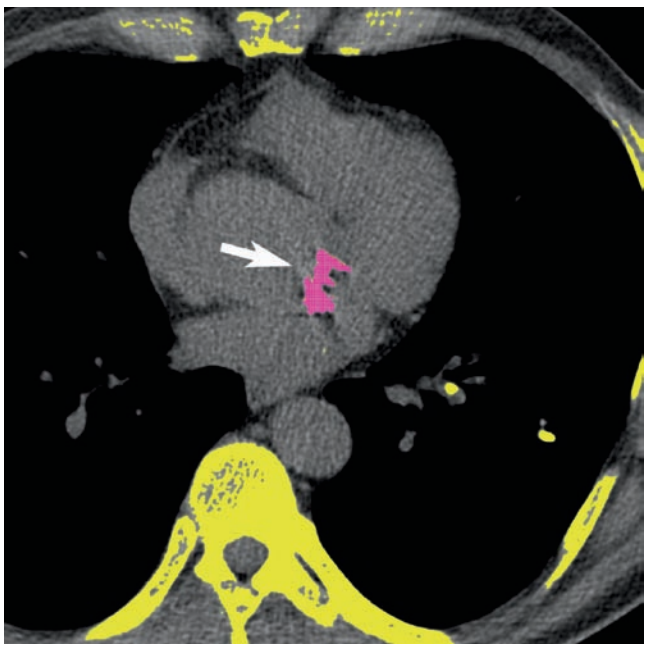

Figure 14.3. Axial, noncontrast CT image in a patient with moderate aortic stenosis, demonstrating the quantification of aortic valve calcium (*arrow*) using the same approach as for coronary calcium scoring. The valvular calcium score ("Agatston") was 2227.

Aortic Regurgitation

CT may be useful in evaluating the mechanism leading to aortic regurgitation (AR). AR caused by degenerative valve disease is characterized by thickened and/or calcified leaflets, and the area of lack of coaptation may be visualized in diastolic phase reconstructions centrally or at the commissures. In cases of AR secondary to enlargement of the aortic root, the regurgitant orifice is typically located centrally (Figure 14.5). Other etiologies that can be depicted include interposition of an intimal flap in cases of dissection, valve distortion or perforation in cases of endocarditis, or leaflet prolapse (observed in dissection and in Marfan syndrome). Regurgitant orifice areas measured by planimetry using MDCT correlate well with echocardiographic parameters of AR severity, such as the vena contracta width and the ratio of regurgitant jet to left ventricular outflow tract height, and allow for the detection of moderate and severe AR with high accuracy [28–30].

Mitral Stenosis

As in the case of aortic valve calcification, the presence of calcium in the mitral annulus is associated with systemic

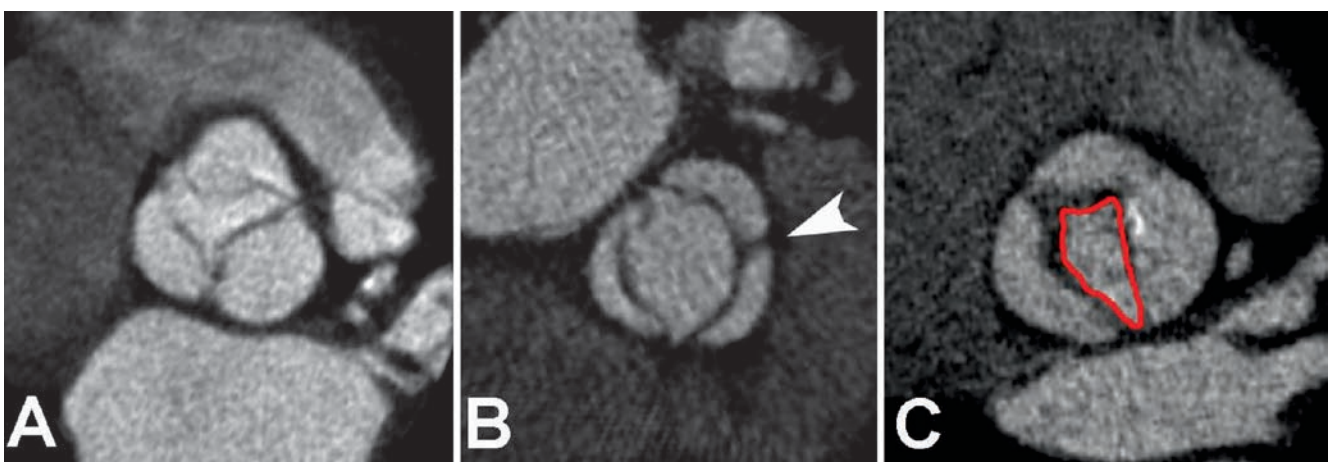

Figure 14.4. Double-oblique systolic reconstructions of contrast-enhanced CT scans showing a tri-leaflet (**a**) and a bicuspid aortic valve (the *arrowhead* indicates the fusion of the right and left coronary sinuses; (**b**) Planimetry of the valve can be performed subsequently (*red contour*, (**c**). The figure shows a bicuspid aortic valve with moderate stenosis (valve area = 1.2 cm^2).

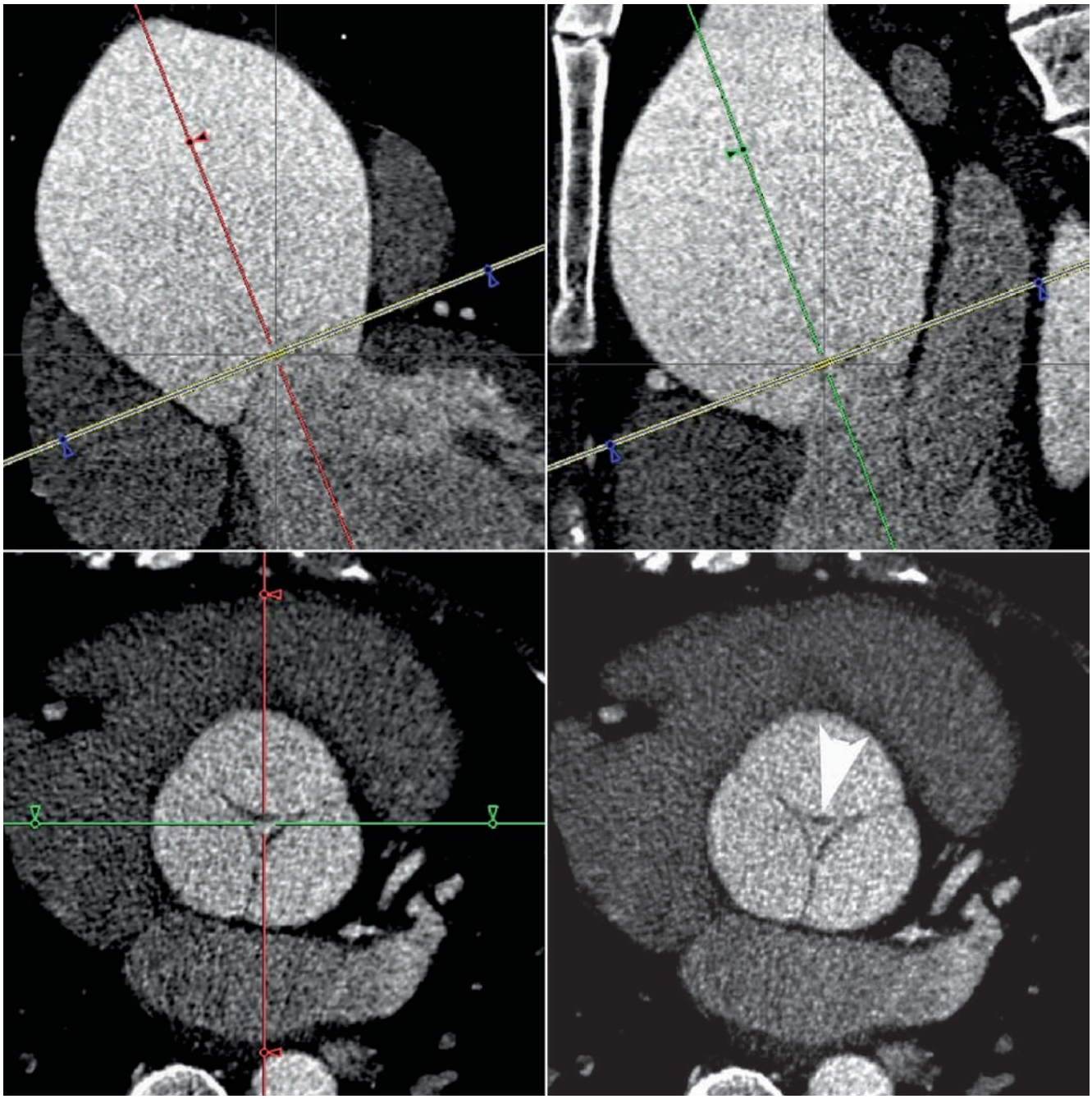

Figure 14.5. Contrast-enhanced MDCT in a patient with an aneurysmal dilated aorta and aortic insufficiency. The valvular plane (*yellow line*) is oriented perpendicular to two orthogonal planes aligned with the ascending aorta (*red* and *green lines*). A large, central area of insufficient leaflet coaptation during diastole (*right lower panel*; *arrowhead*) can be visualized.

atherosclerosis and carries negative prognostic implications. The amount of mitral annular calcium can also be quantified with CT (Figure 14.6), although reproducibility appears to be somewhat lower [15]. In rheumatic mitral stenosis (MS) calcification can extend to the leaflets, commissures, subvalvular apparatus, or even the left atrial wall. MS is often accompanied by marked atrial enlargement involving the appendage. The presence or/absence of thrombus in the left atrial appendage can be determined after contrast administration with very high sensitivity although lower specificity (since slow flow may impair opacification), which may be increased by adding delayed imaging [31, 32]. Planimetry of mitral valve opening by CT provides accurate assessment of MS severity (Figure 14.7) [33].

Mitral Regurgitation

In patients with mitral valve prolapse, CT can demonstrate the presence of leaflet thickening or the degree and location of prolapse (Figure 14.8). In cases of MR secondary to annular enlargement (often accompanying dilated cardiomyopathy), dimensions of the annulus can be accurately quantified, and a central area of insufficient leaflet coaptation may be observed.

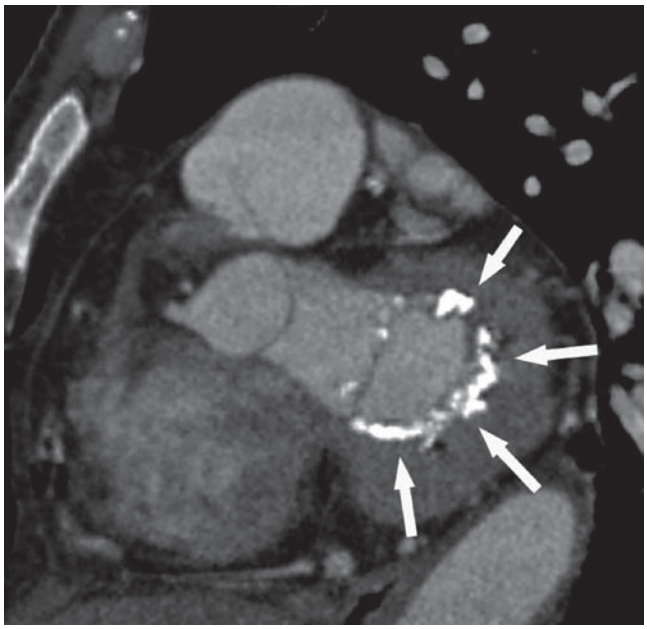

Figure 14.6. Short-axis view at the level of the mitral valve, showing extensive annular calcification (*arrows*).

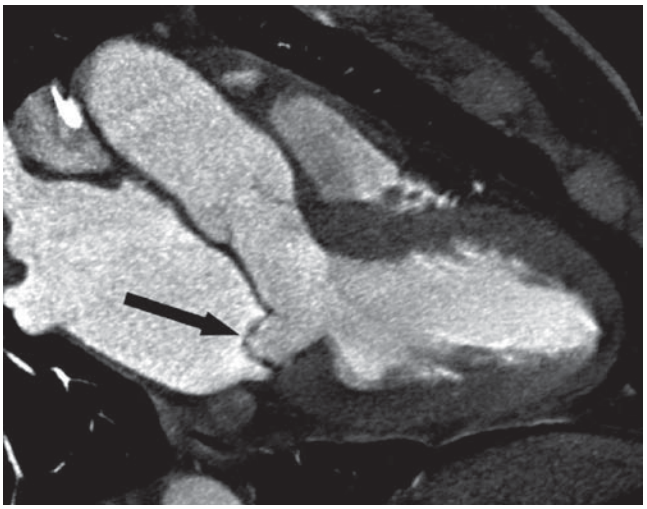

Figure 14.8. End-systolic three-chamber view of the left ventricle demonstrating prolapse of the posterior mitral leaflet (*arrow*).

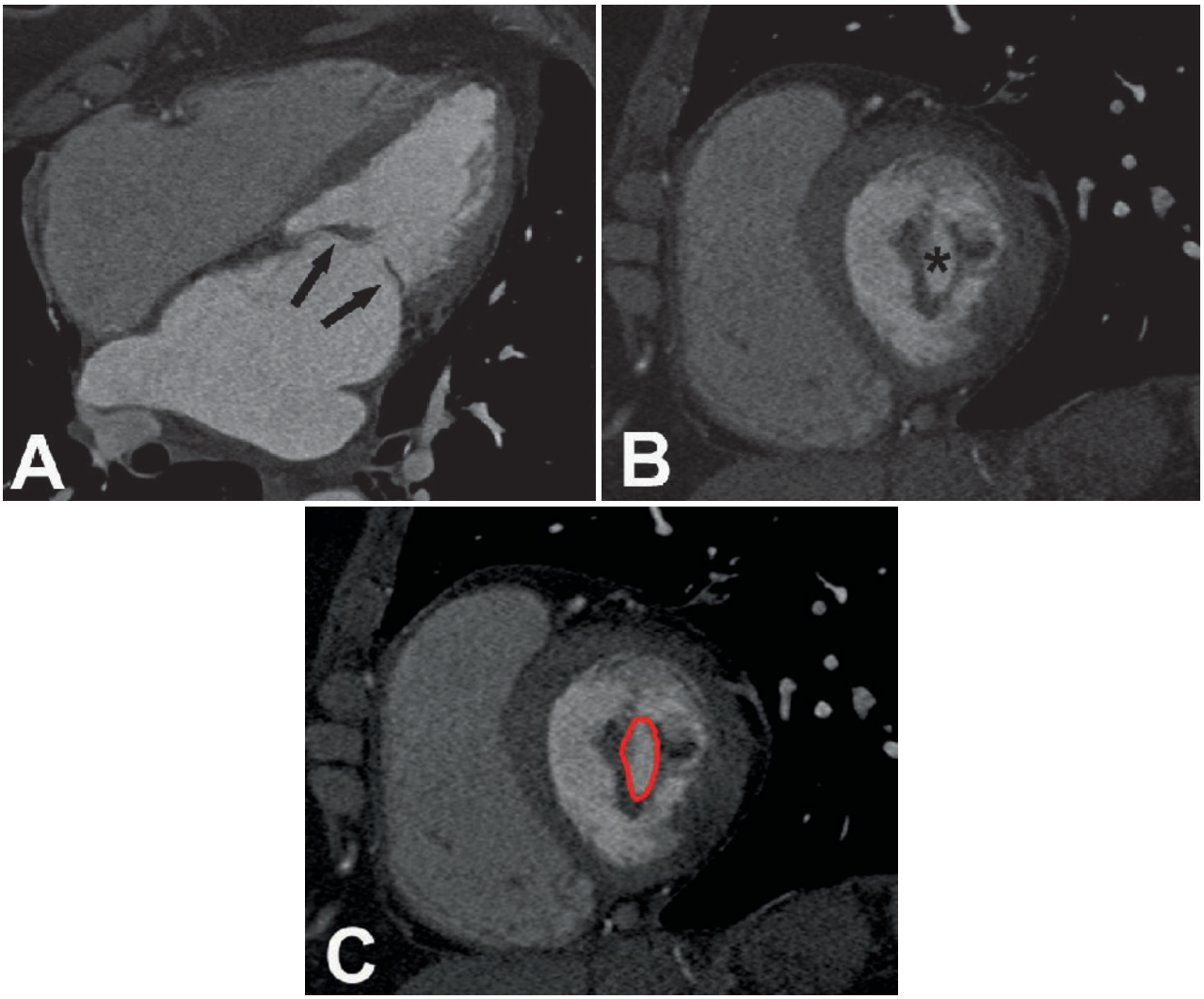

Figure 14.7. Contrast-enhanced CT scan in the four-chamber and short-axis views (**a** and **b**, respectively) from a patient with rheumatic mitral stenosis. The typical thickening and restricted dome-shaped opening of the leaflets can be observed (*arrows* and *asterisk*). Planimetry of the valve (**c**) demonstrated moderate stenosis (*red contour*; area = 1.3 cm^2).

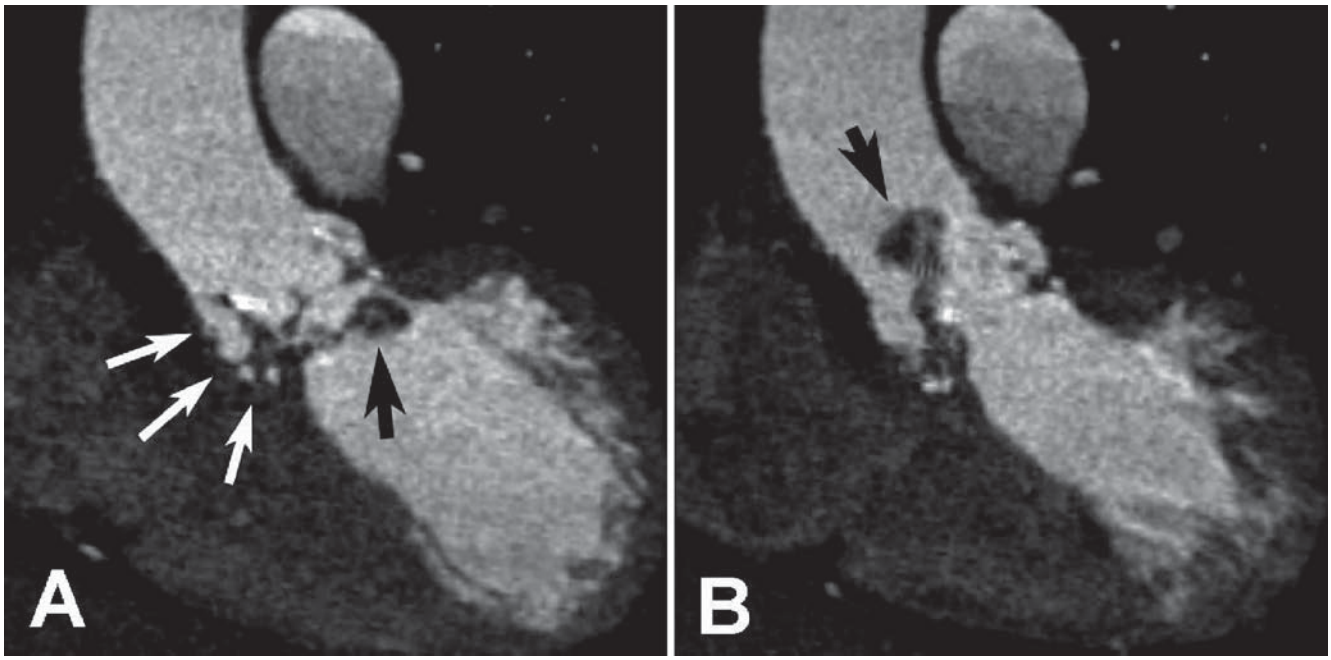

Figure 14.9. Diastolic (**a**) and systolic (**b**) reconstructions of a contrast-enhanced MDCT study in a patient with a bioprosthesis in the aortic position. A large, mobile vegetation that prolapses into the ascending aorta in systole can be noted (*black arrows*). In addition, perivalvular thickening and fluid-filled collections can be noted (*white arrows*) indicating the presence of a perivalular abscess.

Although quantifying MR degree may be difficult, preliminary data suggest that planimetry of the regurgitant orifice by CT correlates well with echocardiographic grading of severity [34]. An alternative approach validated for EBCT includes quantification of cardiac output with the flow mode by the indicator dilution method, and volumetric left ventricular calculations in the cine mode. The regurgitant fraction is obtained from the difference between these two measurements [35].

Infective Endocarditis

The diagnosis of infective endocarditis often relies on the visualization of vegetations, and transthoracic and transesophageal echocardiography are usually superior to CT due to higher temporal resolution. Vegetations are often mobile and tend to be in the atrial aspect in atrioventricular valves and the ventricular aspect in semilunar valves (Figure 14.9). CT can be particularly useful in the demonstration of perivalvular abscesses as fluid-filled collections (Figure 14.9) that may retain contrast in delayed imaging [36]. In a recent study, MDCT correctly identified 26 out of 27 (96%) patients with valvular vegetations and 9 out of 9 (100%) patients with abscesses, which were better characterized by MDCT than with transesophageal echocardiography [37]. In patients with aortic valve endocarditis with highly mobile vegetations, CT may be especially attractive as an alternative to invasive coronary angiography for preoperative evaluation.

Prosthetic Valves

Many of the aforementioned features of native VHD apply also to the evaluation of cardiac bioprostheses. CT is particularly useful for the evaluation of some types of mechanical valves. In prosthesis with two discs, these should open symmetrically (Figure 14.10). In those with a single disc, the angle of opening can also be measured [38]. Finally, heterografts and homografts can be evaluated completely, including the distal anastomosis and the patency of the coronary arteries if these were reimplanted.

Imaging Pearls

Plan ahead; this will allow for imaging protocol optimization if valvular evaluation will be attempted.

If simultaneous assessment of the right heart structures is intended, the contrast protocol should be optimized (Figure 14.11). An initial bolus of 80–100 mL followed by a mixture of contrast and saline (1:1) at 4–5 mL/s will result in adequate coronary evaluation and sufficient right-heart opacification without excessive enhancement. Alternatively, a second infusion of contrast administered at a slower rate (2–3 mL/s) can be employed [12, 13].

Quantification of ventricular end-systolic volumes and the degree of MR and AS requires adequate image quality during systole. It may be necessary to avoid tube current modulation in these cases. Alternatively, the maximal tube output can be timed to end-systole, which will provide adequate depiction of mitral closure and aortic opening, as well as potentially motionless coronary images (particularly at higher heart rates).

If the whole thoracic aorta needs to be imaged (i.e., in cases of aneurysm with associated AR) and the coronary evaluation is not required, using thicker detector collimation will enable reductions in radiation dose and breath-

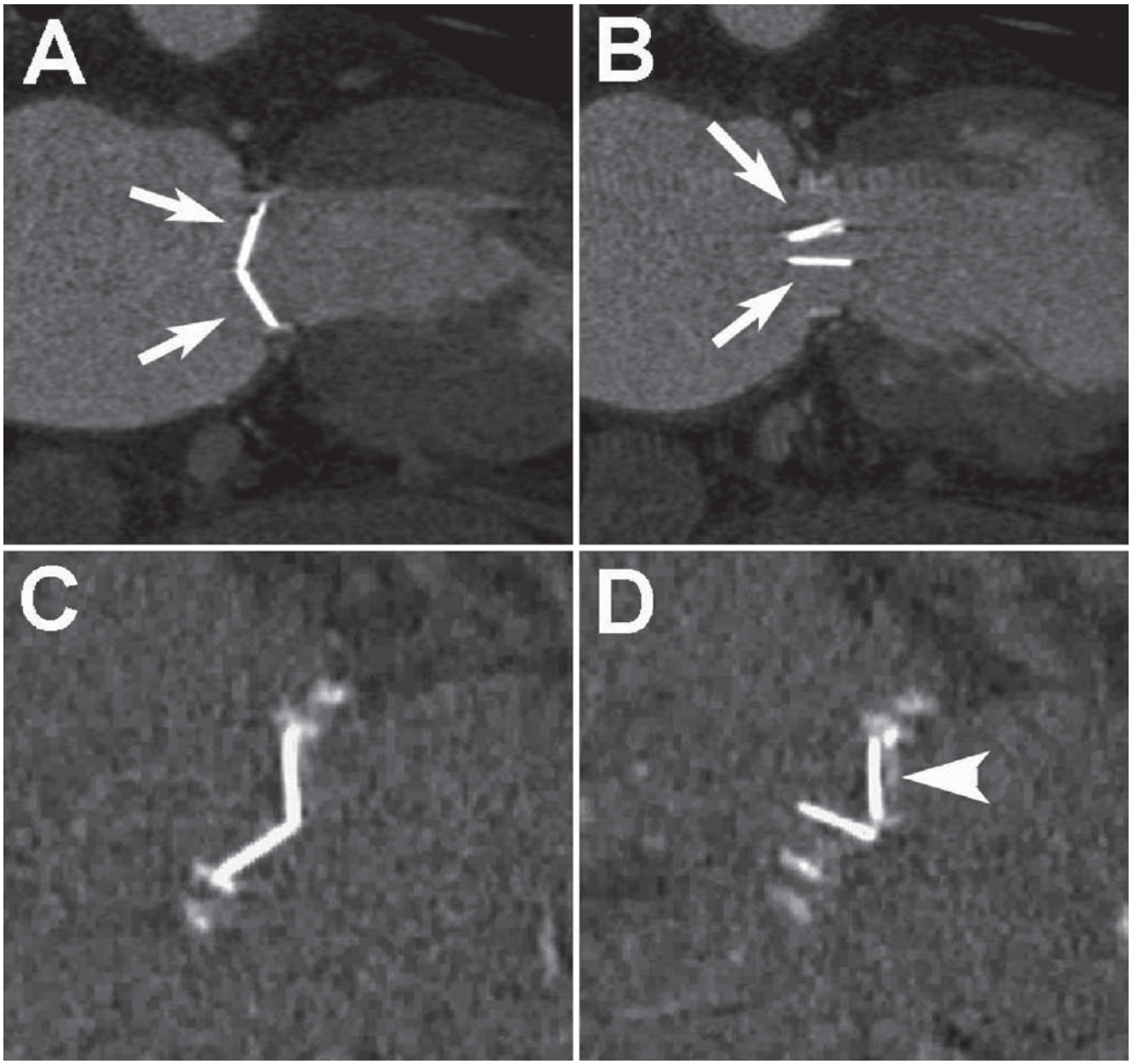

Figure 14.10. Evaluation of mechanical prostheses by CT. The *top row* shows contrast-enhanced images (systole (**a**) diastole (**b**)) of a normal-functioning mechanical prosthesis in the mitral position. The two discs close and open completely and symmetrically (*white arrows*) during the cardiac cycle. Comparable systolic (**c**) and diastolic (**d**) reconstructions of a noncontrast CT evaluation of a dysfunctional mitral prosthesis. One of the discs does not open in diastole (*white arrowhead*). Subsequent surgical intervention demonstrated prosthetic thrombosis.

hold duration. Most patients with VHD can tolerate beta blockers for optimal coronary evaluation. However, caution and smaller doses are recommended in cases with severe degrees of left ventricular dysfunction/dilatation, AS, AR, or pulmonary hypertension.

Atrial fibrillation is common in patients with VHD. It may lead to decrease in image quality and accuracy of valvular and ventricular assessment, although this is typically more significant for evaluation of the coronary arteries.

For the evaluation of ventricular or valvular function with MDCT, reconstructions at every 10% of the RR interval are usually sufficient. In specific cases, a more detailed evaluation of the valve can be obtained by reconstructing images at smaller intervals (i.e., every 5%) in the cardiac phase of interest (for example, during systole for AS) [39]. The combination of cine loops and still frames facilitates the detection of valvular abnormalities.

Variability of the quantification of aortic valve calcium is lowest in mid-diastole [40]. Aortic valvular "Agatston" score ≥1,100 resulted in respective sensitivity and specificity of 93% and 82% for the diagnosis of severe AS [17]. A score >3,700 has a positive predictive value of near 100% [23].

The optimal plane to perform planimetry of the valvular area is parallel to the annulus as determined from two orthogonal double-oblique views perpendicular to the valve plane. The optimal level of that plane is the one showing the smallest area during the phase of maximum valve opening (Figure 14.5).

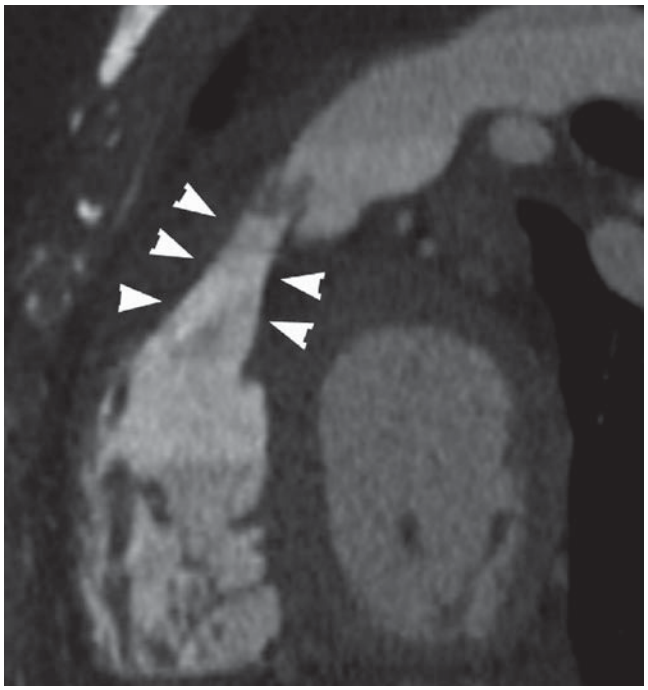

Figure 14.11. Contrast-enhanced CT in a patient with pulmonary infundibula stenosis (*arrowheads*). The contrast protocol was optimized to provide adequate opacification of right heart chambers.

Quantification of the regurgitant volume/fraction from the difference in right and left stroke volumes is only accurate for isolated regurgitant lesions.

A score evaluating leaflet mobility and thickening, subvalvular thickening and calcification, as well as the presence of left atrial thrombus may determine whether MS can be treated percutaneously or surgically. CT can provide useful information of all of these features.

The mitral valve is divided into the anterolateral commissure, posteromedial commissure, anterior leaflet, and posterior leaflet. The leaflets are subdivided into three segments each (A1, A2, and A3; and P1, P2, and P3, from lateral to medial). Determination of which segments are affected and to what degree determines in part the likelihood of successful surgical repair in mitral valve prolapse.

Sharper reconstruction filters and increasing window level of the image display facilitates evaluation of mechanical prosthetic valves (Figure 14.10).

References

1. Nkomo VT, Gardin JM, Skelton TN, Gottdiener JS, Scott CG, Enriquez-Sarano M. Burden of valvular heart diseases: a population-based study. *Lancet*. 2006;368(9540):1005–1011.
2. Bonow RO, Carabello BA, Chatterjee K, et al. 2008 Focused update incorporated into the ACC/AHA 2006 guidelines for the management of patients with valvular heart disease: a report of the American College of Cardiology/American Heart Association Task Force on Practice Guidelines (Writing Committee to Revise the 1998 Guidelines for the Management of Patients With Valvular Heart Disease): endorsed by the Society of Cardiovascular Anesthesiologists, Society for Cardiovascular Angiography and Interventions, and Society of Thoracic Surgeons. *Circulation*. 2008;118(15):e523–e661.
3. Cawley PJ, Maki JH, Otto CM. Cardiovascular magnetic resonance imaging for valvular heart disease: technique and validation. *Circulation*. 2009;119(3):468–478.
4. Orakzai SH, Orakzai RH, Nasir K, Budoff MJ. Assessment of cardiac function using multidetector row computed tomography. *J Comput Assist Tomogr*. 2006;30(4):555–563.
5. Reiter SJ, Rumberger JA, Stanford W, Marcus ML. Quantitative determination of aortic regurgitant volumes in dogs by ultrafast computed tomography. *Circulation*. 1987;76(3):728–735.
6. Boxt LM. CT of valvular heart disease. *Int J Cardiovasc Imaging*. 2005;21(1):105–113.
7. Gilard M, Cornily JC, Pennec PY, et al. Accuracy of multislice computed tomography in the preoperative assessment of coronary disease in patients with aortic valve stenosis. *J Am Coll Cardiol*. 2006;47(10):2020–2024.
8. Meijboom WB, Mollet NR, Van Mieghem CA, et al. Pre-operative computed tomography coronary angiography to detect significant coronary artery disease in patients referred for cardiac valve surgery. *J Am Coll Cardiol*. 2006;48(8):1658–1665.
9. Reant P, Brunot S, Lafitte S, et al. Predictive value of noninvasive coronary angiography with multidetector computed tomography to detect significant coronary stenosis before valve surgery. *Am J Cardiol*. 2006;97(10):1506–1510.
10. Scheffel H, Leschka S, Plass A, et al. Accuracy of 64-slice computed tomography for the preoperative detection of coronary artery disease in patients with chronic aortic regurgitation. *Am J Cardiol*. 2007;100(4):701–706.
11. Russo V, Gostoli V, Lovato L, et al. Clinical value of multidetector CT coronary angiography as a preoperative screening test before non-coronary cardiac surgery. *Heart*. 2007;93(12):1591–1598.
12. Litmanovich D, Zamboni GA, Hauser TH, Lin PJ, Clouse ME, Raptopoulos V. ECG-gated chest CT angiography with 64-MDCT and tri-phasic IV contrast administration regimen in patients with acute non-specific chest pain. *Eur Radiol*. 2008;18(2):308–317.
13. Takakuwa KM, Halpern EJ. Evaluation of a "triple rule-out" coronary CT angiography protocol: use of 64-Section CT in low-to-moderate risk emergency department patients suspected of having acute coronary syndrome. *Radiology*. 2008;248(2):438–446.
14. Rosenhek R, Binder T, Porenta G, et al. Predictors of outcome in severe, asymptomatic aortic stenosis. *N Engl J Med*. 2000;343(9):611–617.
15. Budoff MJ, Takasu J, Katz R, et al. Reproducibility of CT measurements of aortic valve calcification, mitral annulus calcification, and aortic wall calcification in the multi-ethnic study of atherosclerosis. *Acad Radiol*. 2006;13(2):166–172.
16. Koos R, Mahnken AH, Kuhl HP, et al. Quantification of aortic valve calcification using multislice spiral computed tomography: comparison with atomic absorption spectroscopy. *Invest Radiol*. 2006;41(5):485–489.
17. Messika-Zeitoun D, Aubry MC, Detaint D, et al. Evaluation and clinical implications of aortic valve calcification measured by electron-beam computed tomography. *Circulation*. 2004;110(3):356–362.
18. Koos R, Kuhl HP, Muhlenbruch G, Wildberger JE, Gunther RW, Mahnken AH. Prevalence and clinical importance of aortic valve calcification detected incidentally on CT scans: comparison with echocardiography. *Radiology*. 2006;241(1):76–82.
19. Koos R, Mahnken AH, Sinha AM, Wildberger JE, Hoffmann R, Kuhl HP. Aortic valve calcification as a marker for aortic stenosis severity: assessment on 16-MDCT. *AJR Am J Roentgenol*. 2004;183(6):1813–1818.
20. Shavelle DM, Budoff MJ, Buljubasic N, et al. Usefulness of aortic valve calcium scores by electron beam computed tomography as a marker for aortic stenosis. *Am J Cardiol*. 2003;92(3):349–353.
21. Alkadhi H, Wildermuth S, Plass A, et al. Aortic stenosis: comparative evaluation of 16-detector row CT and echocardiography. *Radiology*. 2006;240(1):47–55.
22. Bouvier E, Logeart D, Sablayrolles JL, et al. Diagnosis of aortic valvular stenosis by multislice cardiac computed tomography. *Eur Heart J*. 2006;27(24):3033–3038.
23. Cowell SJ, Newby DE, Burton J, et al. Aortic valve calcification on computed tomography predicts the severity of aortic stenosis. *Clin Radiol*. 2003;58(9):712–716.

24. Feuchtner GM, Dichtl W, Friedrich GJ, et al. Multislice computed tomography for detection of patients with aortic valve stenosis and quantification of severity. *J Am Coll Cardiol*. 2006;47(7):1410–1417.
25. Feuchtner GM, Muller S, Bonatti J, et al. Sixty-four slice CT evaluation of aortic stenosis using planimetry of the aortic valve area. *AJR Am J Roentgenol*. 2007;189(1):197–203.
26. LaBounty TM, Sundaram B, Agarwal P, Armstrong WA, Kazerooni EA, Yamada E. Aortic valve area on 64-MDCT correlates with transesophageal echocardiography in aortic stenosis. *AJR Am J Roentgenol*. 2008;191(6):1652–1658.
27. Lembcke A, Thiele H, Lachnitt A, et al. Precision of forty slice spiral computed tomography for quantifying aortic valve stenosis: comparison with echocardiography and validation against cardiac catheterization. *Invest Radiol*. 2008;43(10):719–728.
28. Alkadhi H, Desbiolles L, Husmann L, et al. Aortic regurgitation: assessment with 64-section CT. *Radiology*. 2007;245(1):111–121.
29. Feuchtner GM, Dichtl W, Muller S, et al. 64-MDCT for diagnosis of aortic regurgitation in patients referred to CT coronary angiography. *AJR Am J Roentgenol*. 2008;191(1):W1–W7.
30. Jassal DS, Shapiro MD, Neilan TG, et al. 64-slice multidetector computed tomography (MDCT) for detection of aortic regurgitation and quantification of severity. *Invest Radiol*. 2007;42(7):507–512.
31. Kim YY, Klein AL, Halliburton SS, et al. Left atrial appendage filling defects identified by multidetector computed tomography in patients undergoing radiofrequency pulmonary vein antral isolation: a comparison with transesophageal echocardiography. *Am Heart J*. 2007;154(6):1199–1205.
32. Hur J, Kim YJ, Lee HJ, et al. Left atrial appendage thrombi in stroke patients: detection with two-phase cardiac CT angiography versus transesophageal echocardiography. *Radiology*. 2009;251(3):683–690.
33. Messika-Zeitoun D, Serfaty JM, Laissy JP, et al. Assessment of the mitral valve area in patients with mitral stenosis by multislice computed tomography. *J Am Coll Cardiol*. 2006;48(2):411–413.
34. Alkadhi H, Wildermuth S, Bettex DA, et al. Mitral regurgitation: quantification with 16-detector row CT–initial experience. *Radiology*. 2006;238(2):454–463.
35. Lembcke A, Borges AC, Dushe S, et al. Assessment of mitral valve regurgitation at electron-beam CT: comparison with Doppler echocardiography. *Radiology*. 2005;236(1):47–55.
36. Gilkeson RC, Markowitz AH, Balgude A, Sachs PB. MDCT evaluation of aortic valvular disease. *AJR Am J Roentgenol*. 2006;186(2):350–360.
37. Feuchtner GM, Stolzmann P, Dichtl W, et al. Multislice computed tomography in infective endocarditis: comparison with transesophageal echocardiography and intraoperative findings. *J Am Coll Cardiol*. 2009;53(5):436–444.
38. Konen E, Goitein O, Feinberg MS, et al. The role of ECG-gated MDCT in the evaluation of aortic and mitral mechanical valves: initial experience. *AJR Am J Roentgenol*. 2008;191(1):26–31.
39. Abbara S, Pena AJ, Maurovich-Horvat P, et al. Feasibility and optimization of aortic valve planimetry with MDCT. *AJR Am J Roentgenol*. 2007;188(2):356–360.
40. Ruhl KM, Das M, Koos R, et al. Variability of aortic valve calcification measurement with multislice spiral computed tomography. *Invest Radiol*. 2006;41(4):370–373.